CHAPTER IV
RESULTS AND DISCUSSION

4.1 Mesoporous TiO_2 Photocatalyst Synthesis

The nanocrystalline mesoporous TiO_2 photocatalyst was synthesized via the surfactant-assisted templating sol-gel method by using TIPT as Ti precursor modified with ACA agent and LAHC as surfactant template. Firstly, TIPT was mixed with ACA, resulting in the change of co-ordination number of Ti atom from 4 to 5, as shown in the following equation. This also causes the change of solution color from colorless to yellow (Brinker *et al.*, 1989). The obtained ACA-modified TIPT is comparatively less active to the moisture in air than the TIPT itself, and is more suitable for the sol-gel synthesis.

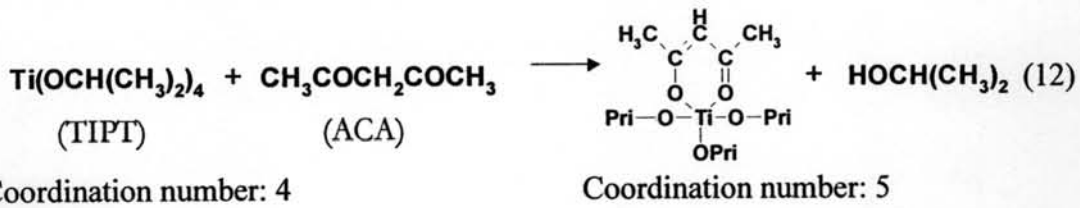

In order to control porosity of the TiO_2, LAHC aqueous solution was added into the TIPT/ACA solution. The precipitation of yellow solution occurred immediately after the aqueous solution addition. Then, the precipitate-containing solution was continuously stirred at 40°C to obtain transparent yellow sol via hydrolysis process, which was resulted from the interaction between the hydrolyzed TIPT molecules and hydrophilic head groups of micellar LAHC. After placing transparent yellow sol into the oven at 80°C, the white gel was formed via condensation process of the modified TIPT molecules attached with the LAHC head groups, and ACA was eliminated as evidenced by the existence of transparent yellow liquid on the gel. During gel incubation for a week, the formation of gel was complete, and the gel was then dried at 80°C to obtain dried TiO_2. The overall sol-gel transition for mesoporous TiO_2 photocatalyst synthesis using TIPT/ACA-LAHC system is shown in Figure 4.1.

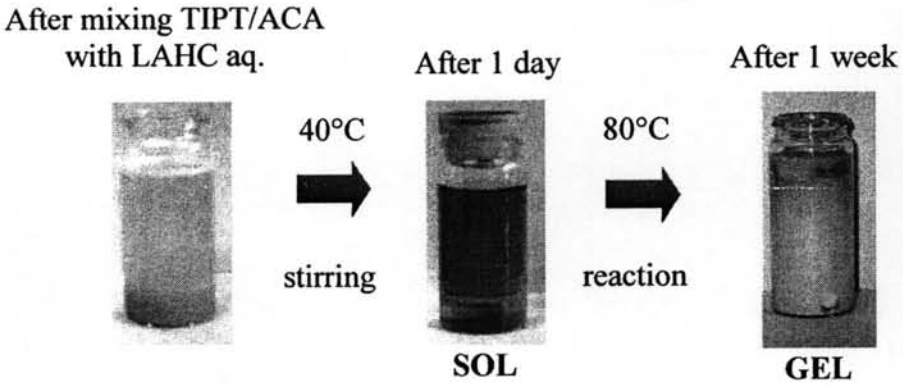

Figure 4.1 Sol-gel transition for mesoporous TiO_2 photocatalyst synthesis.

To obtain mesoporous TiO_2, the dried TiO_2 was calcined at 500°C for 4 h to remove the LAHC template and subsequently produce the desired photocatalyst. The TG-DTA curves were used to study its thermal composition behavior and to obtain a suitable calcination temperature, as shown in Figure 4.2. The DTA curve shows three main exothermic peaks. The details of the position of the exothermic peaks, as well as their corresponding weight loss, are included in Table 4.1. The removal of physisorbed water molecules could contribute to the existence of the first exothermic peak, with its position lower than 150°C. The second exothermic peak between 150-350°C, with its maximum at 282.5°C, is very sharp and narrow, and is attributed to the burnout of the surfactant template. The third exothermic peak between 350-500°C, with its maximum at 411.1°C, is weak and broad, and corresponds to the crystallization process of the photocatalyst and also the removal of chemisorbed water molecules (Hague *et al.*, 1994). From the TG curve, the dominant weight loss of 31.5°C was observed due to the removal of LAHC surfactant template. Since the TG curve shows that weight loss ended at 500°C with total weight loss of 44%, the calcination temperature at this value, i.e. 500°C, was sufficient for removal of the organic surfactant molecules, as well as the crystallization of TiO_2 photocatalyst.

Table 4.1 Thermal decomposition behavior of the synthesized TiO_2 photocatalyst from TG-DTA analysis

Photocatalyst	Position of exothermic peak (°C)			Corresponding weight loss (wt%)			
	1st peak	2nd peak	3rd peak	1st peak	2nd peak	3rd peak	Total
Synthesized TiO_2	76.9	282.5	411.1	2.5	31.5	10.0	44.0

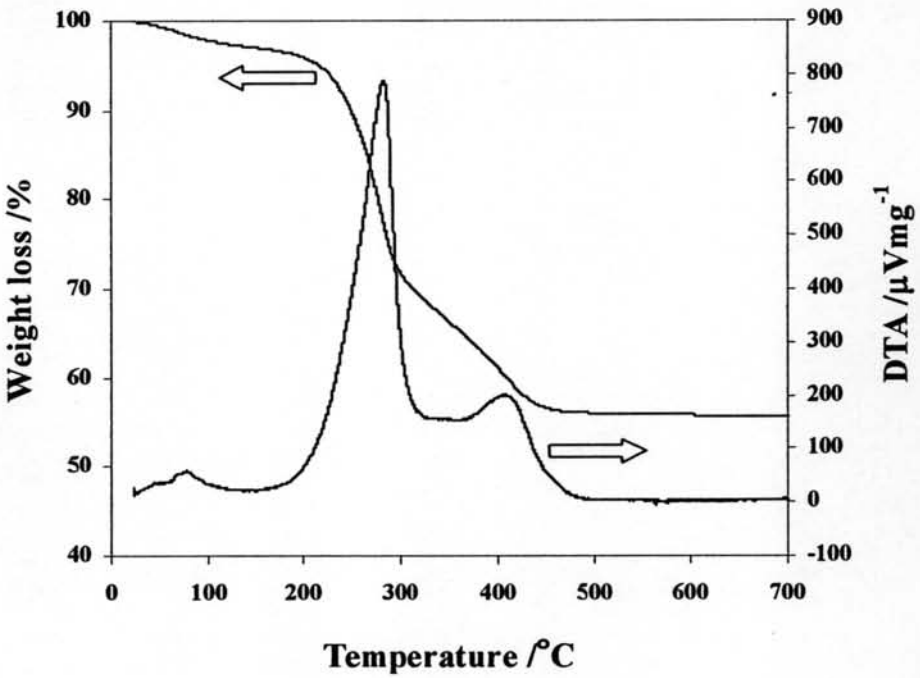

Figure 4.2 TG-DTA curves of the as-synthesized TiO_2 (dried sample).

4.2 N-doped TiO_2 Preparation and Characterizations

To improve the visible light absorption ability of TiO_2, the N-doping was investigated by mixing urea, an N-containing molecule, with the synthesized TiO_2 and commercial Degussa P-25 TiO_2 at various urea:TiO_2 molar ratios and calcining at various calcination temperatures. The results show that synthesized both TiO_2 and commercial Degussa P-25 TiO_2 without N-doping appeared white color, whereas both N-doped synthesized TiO_2 and N-doped commercial Degussa P-25 TiO_2 appeared yellow color.

4.2.1 N_2 Adsorption-Desorption Analysis

In order to verify the mesoporosity of the photocatalyst samples, N_2 adsorption-desorption analysis is very powerful technique normally used. The N_2 adsorption-desorption isotherms of the synthesized TiO_2 and N-doped synthesized TiO_2 exhibited typical IUPAC type IV pattern (Rouquerol *et al.*, 1999), as shown in Figures 4.3 and 4.4, respectively. The hysteresis loop is ascribed to the existence of mesoporous structure (mesopore size between 2-50 nm) in the products. A sharp increase in adsorption volume of N_2 was observed and located in the P/P_0 range of 0.5-0.9. This sharp increase can be assigned to the capillary condensation, indicating good homogeneity of the samples and fairly small pore size since the P/P_0 position of the inflection point is pertained to pore dimension. As illustrated in the inset of Figures 4.3 and 4.4, the pore size distribution obtained from this combined surfactant-assisted sol-gel process is quite narrow, implying good quality of the samples.

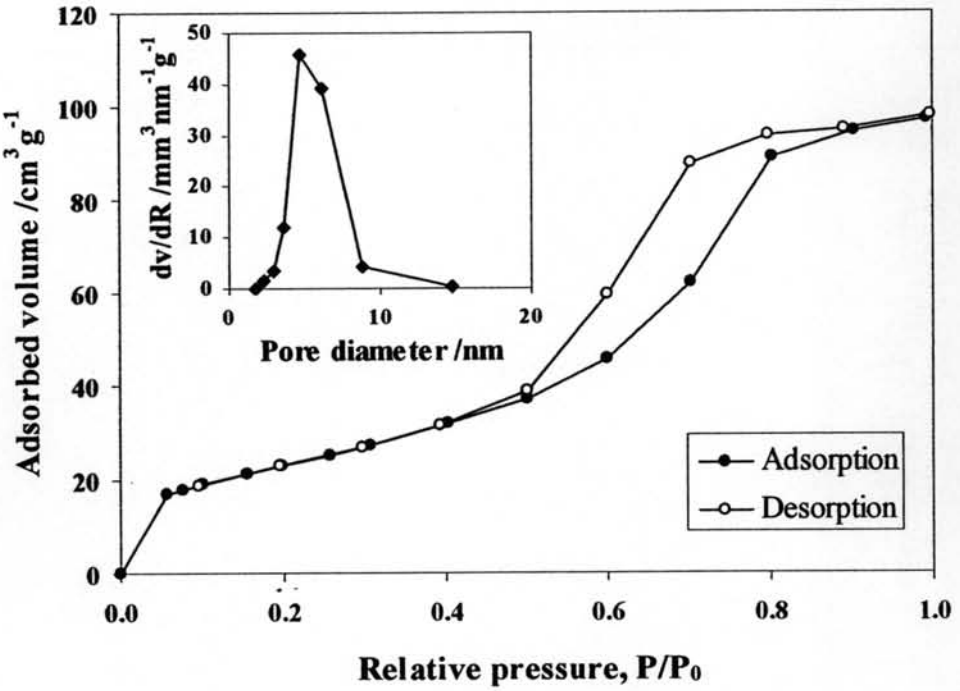

Figure 4.3 N_2 adsorption-desorption isotherm of the synthesized mesoporous TiO_2 calcined at 500°C for 4 h.

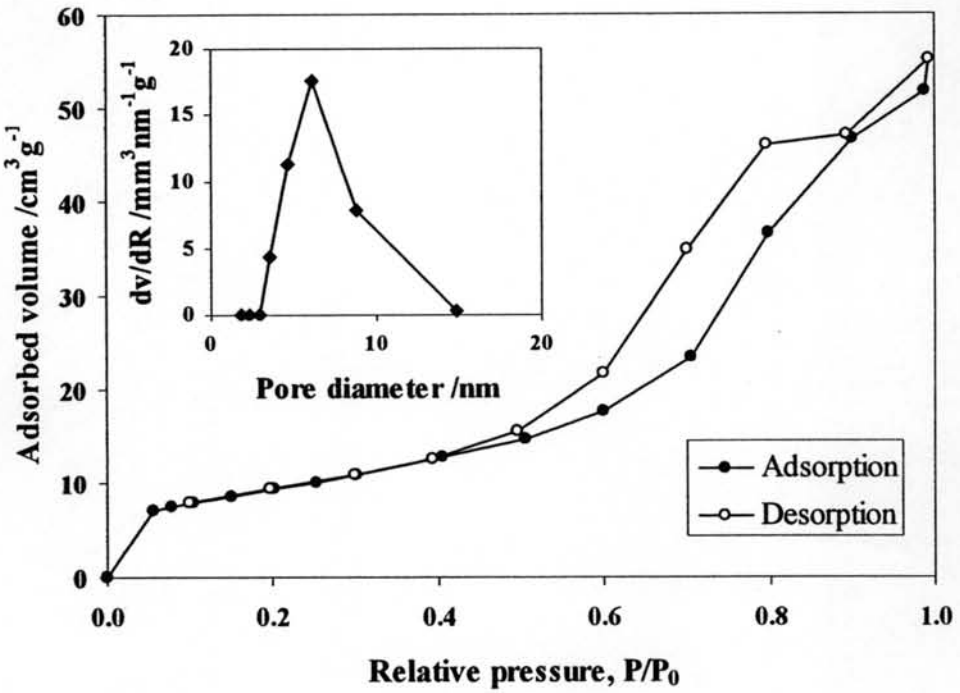

Figure 4.4 N_2 adsorption-desorption isotherm of the N-doped mesoporous TiO_2 prepared at urea:TiO_2 molar ratio of 1:1 and calcined at 250°C for 2 h.

For the commercial Degussa P-25 TiO_2 and N-doped commercial Degussa P-25 TiO_2, N_2 adsorption-desorption isotherms correspond to IUPAC type II pattern (Rouquerol *et al.*, 1999), as depicted in Figures 4.5 and 4.6, respectively. It is apparent that the commercial Degussa P-25 TiO_2 exhibited non-mesoporous characteristic due to the absence of hysteresis loop. No capillary condensation of N_2 into the pore was observed since the desorption isotherm was insignificantly different from the adsorption one. The pore size distribution of commercial Degussa P-25 TiO_2, as shown in the inset of Figures 4.5 and 4.6, is quite broad. This results show that the pore size of commercial Degussa P-25 TiO_2 and N-doped commercial Degussa P-25 TiO_2 are quite large in average since their pore size distributions not only exist in the mesoporous region (mesopore size between 2-50 nm) but also mostly cover the macropore region (macropore size > 50 nm). Therefore, the surface area of commercial Degussa P-25 TiO_2 was consequently observed to be less than the synthesized mesoporous TiO_2.

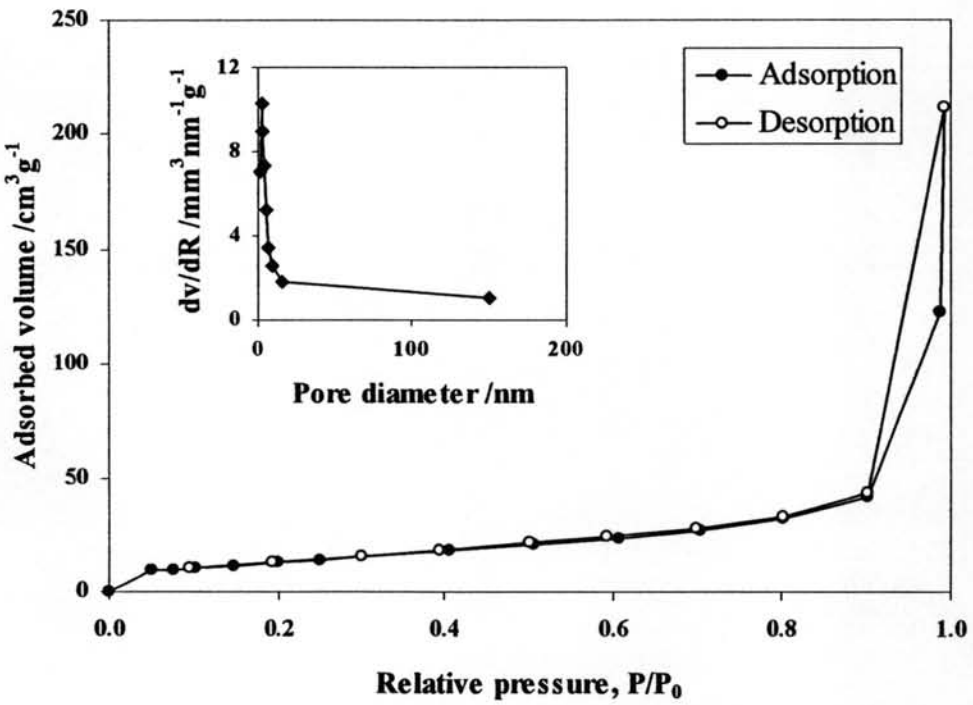

Figure 4.5 N_2 adsorption-desorption isotherm of the commercial Degussa P-25 TiO_2.

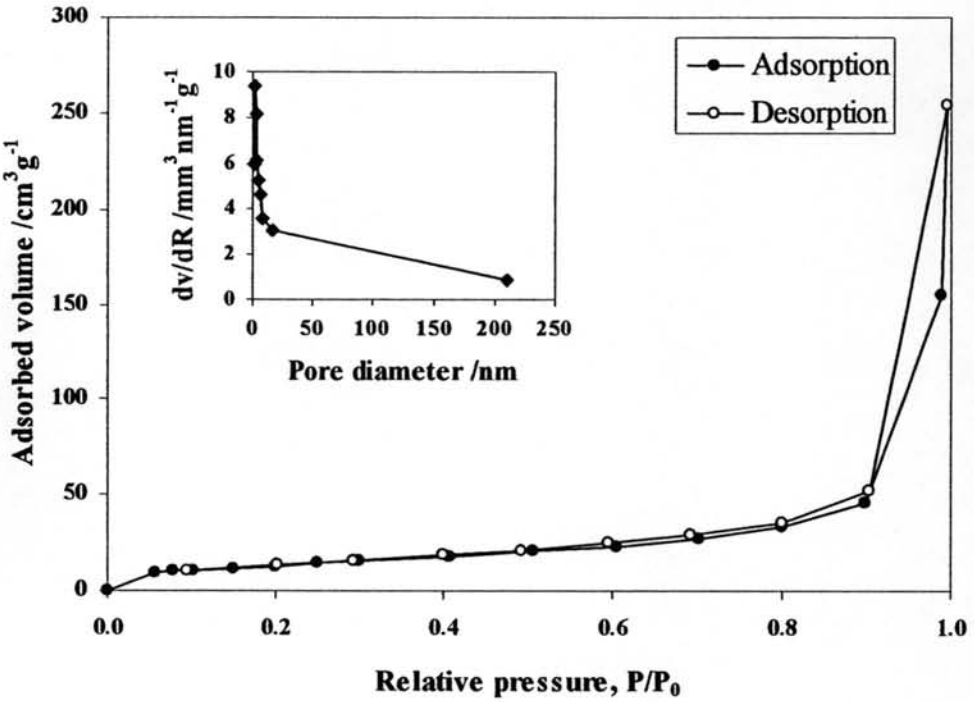

Figure 4.6 N_2 adsorption-desorption isotherm of the N-doped commercial Degussa P-25 TiO_2 prepared at urea:TiO_2 molar ratio of 0.5:1 and calcined at 250°C for 2 h.

4.2.2 Textural Property Analysis

The experimental results on textural properties of the photocatalysts, including BET surface area, mean pore diameter, and total pore volume, are shown in Table 4.2. For all N-doped mesoporous and N-doped commercial Degussa P-25 TiO_2 photocatalysts, the surface area tended to decrease with increasing the urea:TiO_2 molar ratio at all calcination temperatures. For the N-doped mesoporous TiO_2, of which the isotherm exhibited typical IUPAC type IV, the mean pore diameter was quite similar to pure mesoporous TiO_2, however the total pore volume decreased with increasing the urea:TiO_2 molar ratio. For the commercial Degussa P-25 TiO_2, the mean pore diameter and total pore volume are always not reported because it contains a large portion of macropore, which possesses very broad pore size distribution with the pore diameter larger than 50 nm, up to 200-250 nm.

Table 4.2 Summary of textural properties of the TiO_2 photocatalysts without and with N-doping prepared at various conditions

Calcination temperature/ °C	Urea:TiO_2 molar ratio	BET surface area /m^2g^{-1}	Mean pore diameter/nm	Total pore volume/cm^3g^{-1}
	Pure mesoporous TiO_2	110.30	6.114	0.185
200	0.5:1	78.14	6.150	0.136
	1:1	35.36	6.156	0.070
	3:1	22.12	4.619	0.044
250	0.5:1	82.83	6.146	0.155
	1:1	38.52	6.129	0.080
	3:1	23.45	6.140	0.049
300	0.5:1	75.78	6.150	0.147
	1:1	73.98	6.161	0.137
	3:1	22.86	6.104	0.053
	Pure Degussa P-25 TiO_2	69.35	- [(a)]	- [(a)]
200	0.5:1	54.96	- [(a)]	- [(a)]
	1:1	53.26	- [(a)]	- [(a)]
	3:1	17.63	- [(a)]	- [(a)]
250	0.5:1	50.66	- [(a)]	- [(a)]
	1:1	44.63	- [(a)]	- [(a)]
	3:1	20.77	- [(a)]	- [(a)]
300	0.5:1	51.40	- [(a)]	- [(a)]
	1:1	26.21	- [(a)]	- [(a)]
	3:1	24.22	- [(a)]	- [(a)]

[(a)] N_2 adsorption-desorption isotherm corresponds to IUPAC type II pattern.

4.2.3 UV-Vis Spectroscopy

UV-Vis spectroscopy was used to investigate the light absorption capability of the photocatalysts. The changes in UV-Vis spectra of N-doped mesoporous TiO_2 with different N-doping content are exemplified in Figure 4.7.

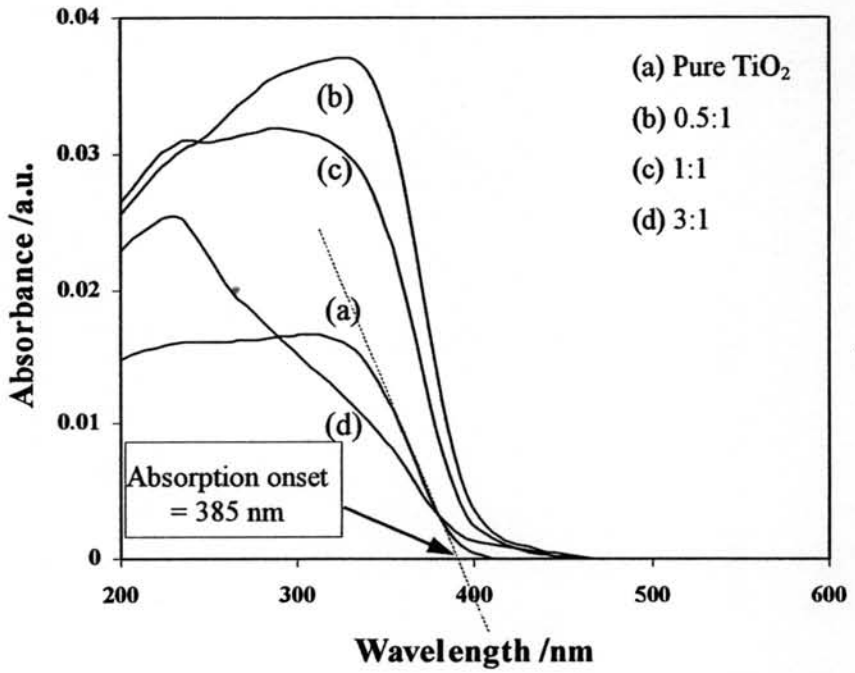

Figure 4.7 UV-Vis spectra of (a) pure nanocrystalline mesoporous TiO_2 and (b)-(d) N-doped mesoporous TiO_2 with different urea:TiO_2 molar ratios of 0.5:1, 1:1, and 3:1, respectively, prepared at calcination conditions of 250°C for 2 h.

From Figure 4.7, the absorption band of pure mesoporous TiO_2 is in the range of 200-400 nm. The strong absorption band at low wavelength in the spectra indicated the presence of Ti species as tetrahedral Ti^{4+}. This absorption band is generally associated with the electronic excitation of the valence band O2p electron to the conduction band Ti3d level (Fuerte *et al.*, 2002). Its absorption onset is approximately at 385 nm, which corresponds to the energy band gap of anatase TiO_2 of 3.2 eV. For the N-doped mesoporous TiO_2 as shown in Figure 4.7, the absorption band shifts to wavelength longer than 400 nm, which is in the range of visible region. Therefore, the N-doping was proved to improve the visible light absorption of TiO_2.

For the N-doped commercial Degussa P-25 TiO_2, the UV-Vis spectra are exemplified in Figure 4.8.

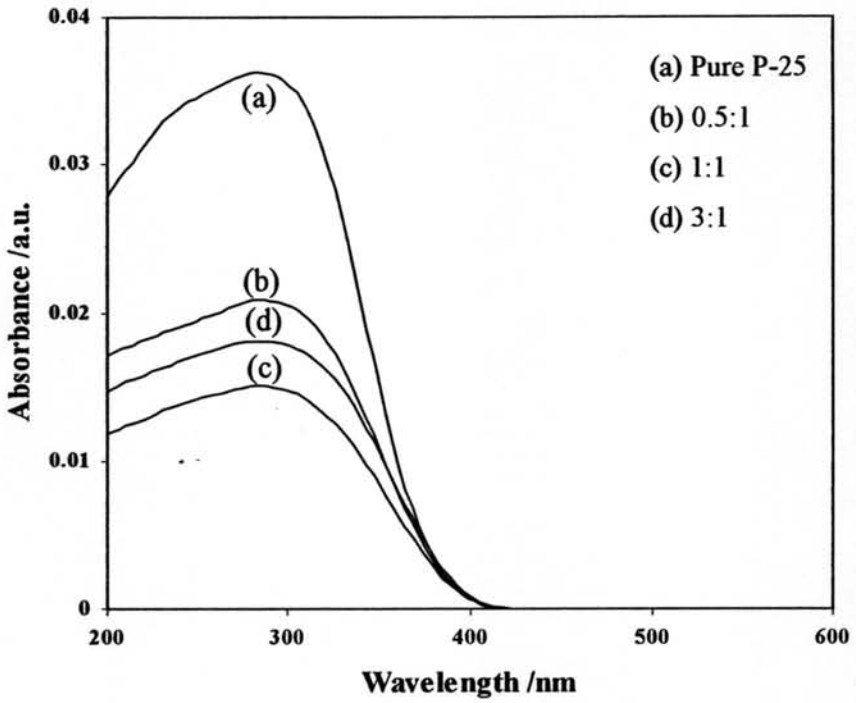

Figure 4.8 UV-Vis spectra of (a) commercial Degussa P-25 TiO_2 and (b)-(d) N-doped commercial Degussa P-25 TiO_2 with different urea:TiO_2 molar ratios of 0.5:1, 1:1, and, 3:1, respectively, prepared at calcination conditions of 250°C for 2 h.

The absorption onset of pure commercial Degussa P-25 TiO_2 begins at the wavelength longer than 400 nm, which simply indicates that it can absorb visible light by itself in spite of the absence of N-doping. This result is because the commercial Degussa P-25 TiO_2 possesses both anatase and rutile phases, as shown by XRD patterns in the next part. Their energy band gap is approximately 3.2 and 3.0 eV for anatase and rutile TiO_2, respectively, which can absorb both UV and visible regions. The UV-Vis results of TiO_2 with various N content show that the visible light absorption onsets between pure and N-doped commercial Degussa P-25 TiO_2 are slightly different.

4.2.4 X-ray Diffraction Analysis

The XRD patterns of the N-doped mesoporous TiO_2 prepared at different urea:TiO_2 molar ratios and calcination temperatures are shown in Figure 4.9, comparing with the pure mesoporous TiO_2 photocatalyst, whereas those of N-doped commercial Degussa P-25 TiO_2 prepared at different urea:TiO_2 molar ratios and calcination temperatures are shown in Figure 4.10, also comparing with the pure commercial Degussa P-25 TiO_2 .

As shown in Figure 4.9, all samples of N-doped mesoporous TiO_2 prepared at urea:TiO_2 molar ratio of 0.5:1 (Figure 4.9(b), (e), and (h)), regardless of calcination temperatures, showed quite similar XRD diffractograms with the pure mesoporous TiO_2 (Figure 4.9(a)). The dominant peaks at 2θ of about 25.2, 37.9, 47.8, 53.8, and 55.0°, which represent the indices of (1 0 1), (0 0 4), (2 0 0), (1 0 5), and (2 1 1) planes (JCPDS Card No. 21-1272), (Smith, 1960), respectively, are conformed to crystalline structure of anatase TiO_2. At temperature of 200°C, the biuret formation was first clearly observed at the urea:TiO_2 molar ratio of 3:1, as shown in Figure 4.9(d). The biuret was also found at the urea:TiO_2 molar ratio of 1:1, but very small amount due to comparatively low peak intensity at this temperature (Figure 4.9(c)). The similar tendency of biuret formation was observed at the temperature of 250°C for the urea:TiO_2 molar ratios of both 1:1 and 3:1 (Figure 4.9(f) and (g)). In addition, the cyanuric acid was apparently formed at this temperature. At 300°C, the biuret formation was not observed at the molar ratio of 1:1 (Figure 4.9(i)) because of the high calcination temperature. At the molar ratio of 3:1 (Figure 4.9(j)), the cyanuric acid formation was highly observed, and the biuret formation was observed with relatively less amount when compared to the temperature of 250°C at the same ratio. These results indicate that the cyanuric acid was formed at temperature higher than 200°C, above which the biuret started decomposing.

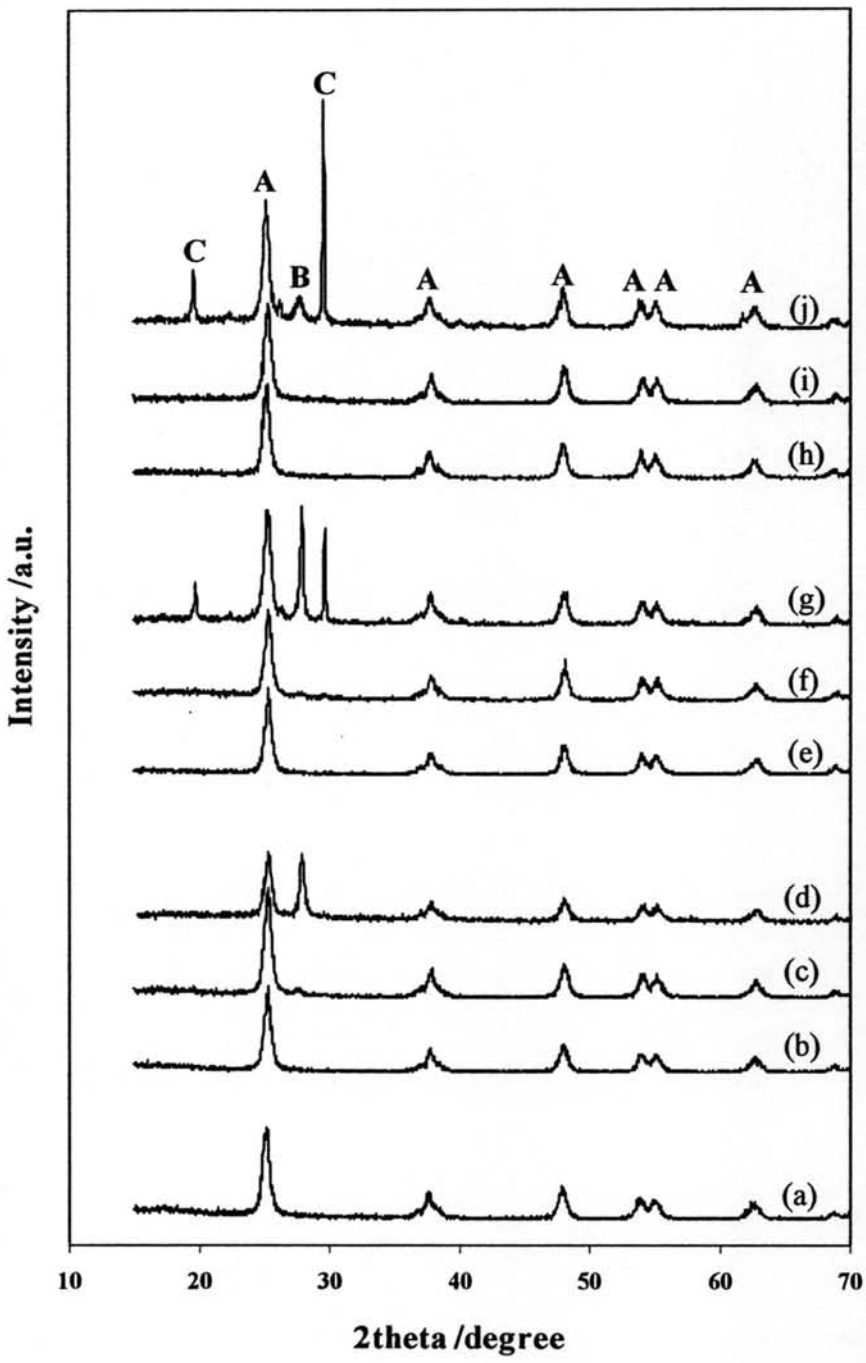

Figure 4.9 XRD patterns of (a) pure mesoporous TiO_2, and (b)-(d) N-doped mesoporous TiO_2 with different urea:TiO_2 molar ratios of 0.5:1, 1:1, and, 3:1, respectively, prepared at calcination conditions of 200°C for 2 h, (e)-(g) urea:TiO_2 molar ratios of 0.5:1, 1:1, and, 3:1, respectively, at 250°C for 2 h, (h)-(j) urea:TiO_2 molar ratios of 0.5:1, 1:1, and, 3:1, respectively, at 300°C for 2 h (A: Anatase TiO_2, B: Biuret, C: Cyanuric acid).

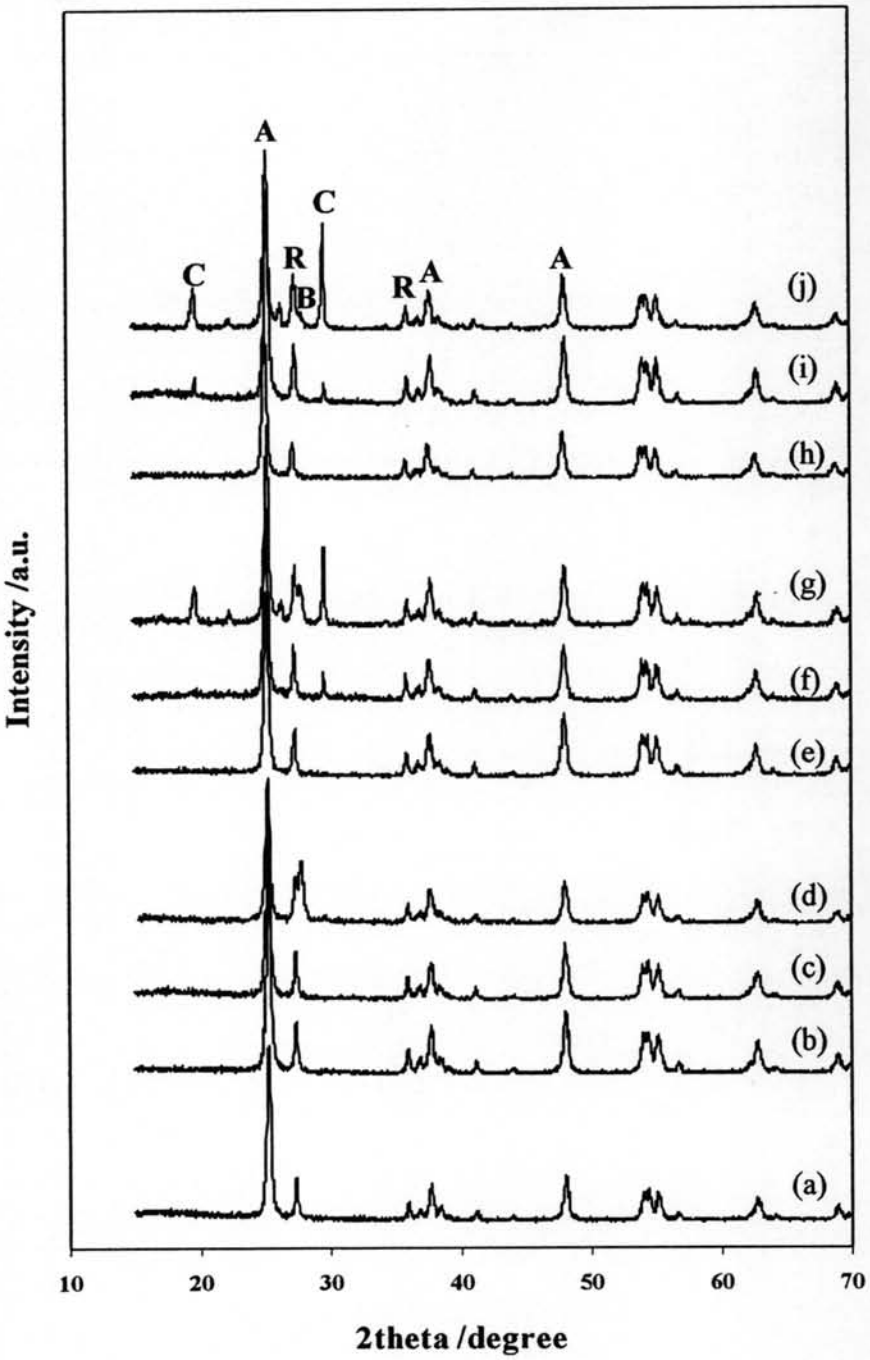

Figure 4.10 XRD patterns of (a) commercial Degussa P-25 TiO_2, (b)-(d) N-doped commercial Degussa P-25 TiO_2 with different urea:TiO_2 molar ratios of 0.5:1, 1:1, and, 3:1, respectively, prepared at calcination conditions of 200°C for 2 h, (e)-(g) urea:TiO_2 molar ratios of 0.5:1, 1:1, and, 3:1, respectively, at 250°C for 2 h, (h)-(j) urea:TiO_2 molar ratios of 0.5:1, 1:1, and, 3:1, respectively, at 300°C for 2 h (A: Anatase TiO_2, R: Rutile TiO_2, B: Biuret, C: Cyanuric acid).

Schaber *et al.* (1999) explained about the decomposition of urea that the urea pyrolysis reaction can be decomposed to many components depending on temperature. Two main components are biuret and cyanuric acid. Upon increasing temperature, biuret production is occurred at approximate temperature between 150 and 250°C. Cyanuric acid formation is then occurred in consecutive order at approximate temperature between 190 and 350°C.

The formations of biuret and cyanuric acid due to urea composition are shown in the following mechanism:

At temperature between 150 and 250°C

$$\underset{\text{urea}}{H_2N\text{-}CO\text{-}NH_2\ (m)} + \text{heat} \longrightarrow \underset{\text{ammonium iso-cyanate}}{NH_4^+NCO^-\ (m)} \qquad (13)$$

$$\underset{\text{ammonium iso-cyanate}}{NH_4^+NCO^-\ (m)} \longleftrightarrow \underset{\text{ammonia}}{NH_3\ (g)} + \underset{\text{iso-cyanic acid}}{HNCO\ (g)} \qquad (14)$$

$$\underset{\text{urea}}{H_2N\text{-}CO\text{-}NH_2\ (m)} + \underset{\text{iso-cyanic acid}}{HNCO\ (g)} \longleftrightarrow \underset{\text{biuret}}{H_2N\text{-}CO\text{-}NH\text{-}CO\text{-}NH_2\ (s)} \qquad (15)$$

At temperature between 190 and 350°C

$$\underset{\text{iso-cyanic acid}}{3HNCO\ (g)} \longrightarrow \underset{\text{cyanuric acid}}{C_3O_3N_3H_3\ (s)} \qquad (16)$$

$$\underset{\text{biuret}}{2H_2N\text{-}CO\text{-}NH\text{-}CO\text{-}NH_2\ (m)} \longrightarrow \underset{\text{cyanuric acid}}{C_3O_3N_3H_3\ (s)} + \underset{\text{iso-cyanic acid}}{HNCO\ (g)} + \underset{\text{ammonia}}{NH_3\ (g)} \qquad (17)$$

The expressed mechanism exactly correspond to the effect of calcination temperature on the formation of impurities (biuret and cyanuric acid) at high urea:TiO_2 molar ratio of 3:1 that the peak responsible for biuret formation was

firstly observed at 200°C, and its intensity increased when increasing the calcination temperature to 250°C. With further increasing the temperature to 300°C, the amount of biuret formed was decreased. In the meantime, cyanuric acid formation was firstly denoted at 250°C and mostly occurred at 300°C.

For the XRD patterns of N-doped commercial Degussa P-25 TiO_2 as shown in Figure 4.10, the dominant peaks at 2θ of about 27.4, 36.1, 41.2, and 54.3°, which represent the indices of (1 1 0), (1 0 1), (1 1 1), and (2 1 1) planes (JCPDS Card No. 21-1276), (Smith, 1960), respectively, indicate the presence of rutile phase, in addition to the presence of anatase phase. The formation of biuret and cyanuric acid were observed in the same trend with N-doped mesoporous (Figure 4.9). The main difference between mesoporous TiO_2 and commercial Degussa P-25 TiO_2 photocatalysts was that the commercial Degussa P-25 TiO_2 possesses mixed phase of anatase (76.5%) and rutile (23.5%), of which the phase composition was calculated by Eq. (16) and (17) (Spurr and Myers, 1957).

$$W_R = [1+0.8I_A/I_R]^{-1} \quad (18)$$

$$W_A = 1- W_R \quad (19)$$

where I_A and I_R represent integrated intensities of anatase (1 0 1) and rutile (1 1 0) diffraction peaks, respectively. And, W_A and W_R represent phase compositions of anatase and rutile, respectively.

4.2.5 XPS Analysis

The oxidation states and surface compositions of N, O, and Ti for N-doped mesoporous TiO_2 and N-doped commercial Degussa TiO_2 were analyzed by XPS. The results for N-doped mesoporous TiO_2 with urea:TiO_2 molar ratio of 1:1 prepared at calcination temperature of 250°C are exemplified in Figure 4.11.

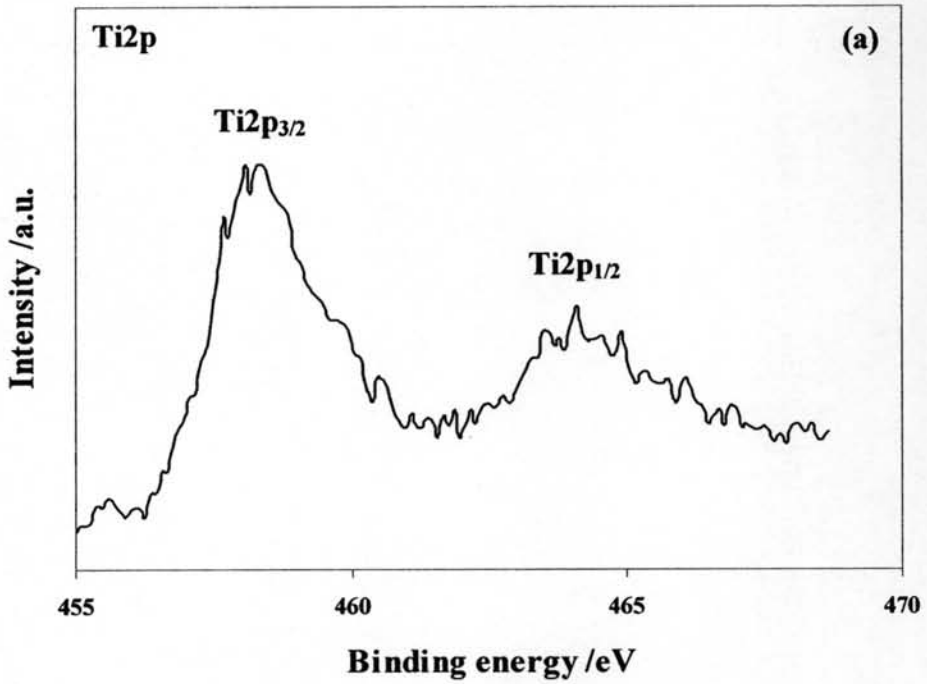
Ti2p
(a)
Ti2p3/2
Ti2p1/2
Intensity /a.u.
455
460
465
470
Binding energy /eV

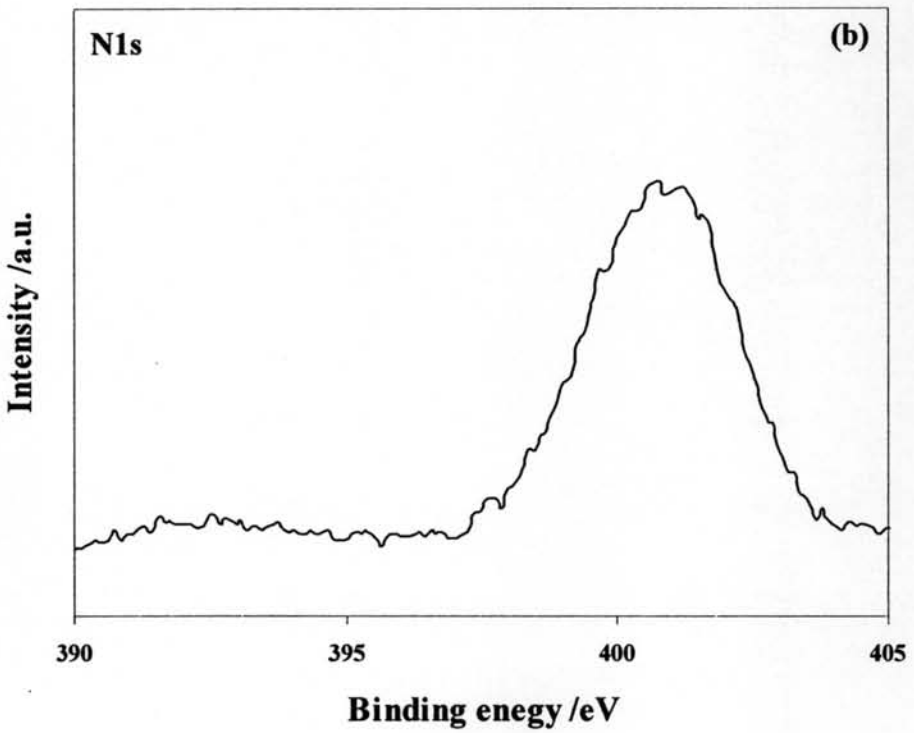
N1s
(b)
Intensity /a.u.
390
395
400
405
Binding enegy /eV

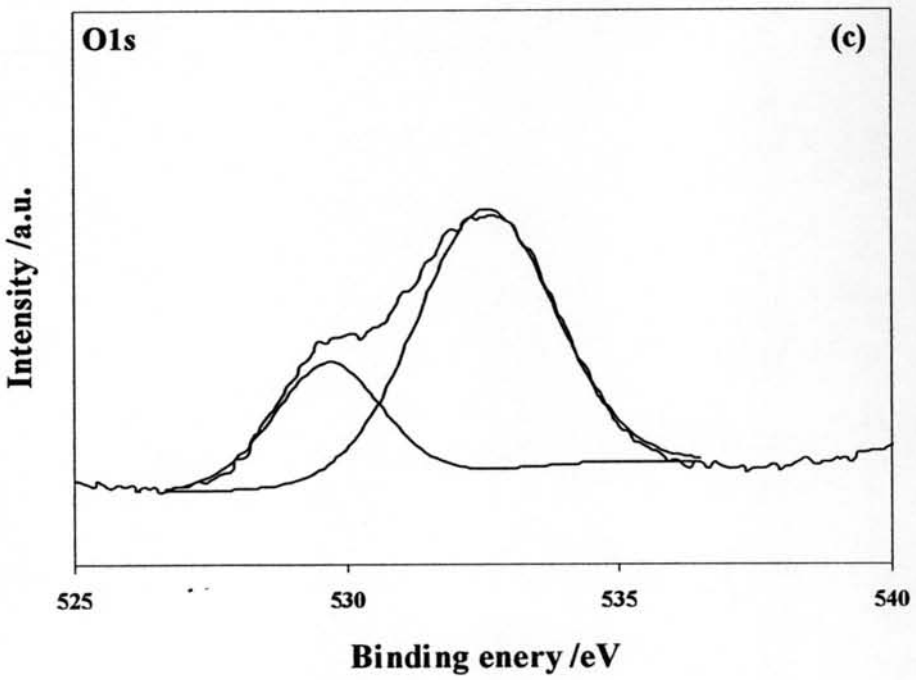

Figure 4.11 XPS spectra of (a) Ti, (b) N, and (c) O for N-doped mesoporous TiO_2 with the urea:TiO_2 molar ratio of 1:1 prepared at calcination temperature of 250°C.

Figure 4.11(a) represents a typical XPS spectrum of Ti. The Ti2p spectrum appeared at 458.4 and 464.0 eV, which correspond to $Ti2p_{3/2}$ and $Ti2p_{1/2}$ levels, respectively. The peaks can denote to Ti^{4+} oxidation state. Figure 4.11(b) shows that the N1s spectrum appeared at 401.8 eV, which can be ascribed to molecularly chemisorbed nitrogen. Figure 4.11(c) shows that the O1s (mesoporous TiO_2) spectrum appeared at 529.7 eV, which is typical for Ti-O-Ti environment and agrees with O1s binding energy for TiO_2 molecule (Zhang *et al*, 2006), and at 532.5 eV, which is typical for Ti-O-H environment of the hydroxyl group on the photocatalyst surface (Yu *et al*, 2005).

Nosaka *et al.* (2005) also investigated the N-doped TiO_2 photocatalyst with XPS analysis and observed that N1s spectrum appeared at both 396.7 and 401.8 eV, representing atomically substitutional nitrogen and molecularly chemisorbed nitrogen with comparatively low signal for the former. Although the N1s with binding energy of 396.7 eV was not clearly observed for the samples in this study, it is believed to exist with low content. It has been analyzed that the peak at 396.7 eV is

typical for N bond to Ti atoms, and the signal around 402 eV is typical for N bound to O, C, or N atoms. The surface nitrogen composition of all investigated N-doped TiO_2 is summarized in Table 4.3.

Table 4.3 The summary of surface N content of N-doped photocatalyst

Calcination temperature /°C	Urea:mesoporous TiO_2 molar ratio	Surface N content /wt%	Urea:Degussa P-25 molar ratio	Surface N content /wt%
	Pure mesoporous TiO_2	4.72	Pure Degussa P-25 TiO_2	2.59
200	0.5:1	5.77	0.5:1	3.96
	1:1	20.11	1:1	5.01
	3:1	21.28	3:1	7.73
250	0.5:1	8.70	0.5:1	3.21
	1:1	26.23	1:1	4.68
	3:1	32.61	3:1	7.93
300	0.5:1	7.11	0.5:1	2.35
	1:1	11.23	1:1	2.91
	3:1	30.25	3:1	7.17

The existence of surface nitrogen on the synthesized pure mesoporous TiO_2 may be due to the imperfect removal of LAHC surfactant template. For the pure commercial Degussa P-25 TiO_2, the presence of surface nitrogen is plausibly because of their production technique via spray combustion. It seems to be that when calcining TiO_2 photocatalyst in air atmosphere containing N_2 of 78%, the photocatalyst can be inevitably N-doped. For the N-doped mesoporous TiO_2, it can be seen that at all urea:TiO_2 molar ratios, the surface N content increased with increasing the calcination temperature from 200 to 250°C but decreased with further increasing the calcination temperature to 300°C, as shown in Table 4.3. The trend of surface N content for N-doped mesoporous TiO_2 is quite different from that for N-doped Degussa P-25 TiO_2, of which at all urea:TiO_2 molar ratios, the surface N content tended to decrease with increasing the calcination temperature from 200-

300°C. These results can be probably related to their pore characteristics. As the pore size of the synthesized TiO_2 entirely exists in mesopore region, the formed N-containing compounds at 250°C, i.e. biuret and cyanuric acid, could not leave the pore due to pore size limitation, resulting in higher surface N content observed. With increasing the temperature to 300°C, these compounds can be more easily thermally released from the pore structure at this high temperature. In contrast to the pore size of the Degussa P-25 TiO_2, which is almost present in large macropore region, any compounds formed can be simultaneously released due to thermal removal more easily at higher temperature.

Moreover, it can be found that at any calcination temperature, the surface N content increased with increasing the urea:TiO_2 molar ratio for both the mesoporous TiO_2 and commercial Degussa P-25, reasonably due to the presence of higher amount of available urea molecules as to increase the doping capability. When comparing between these two types of TiO_2, it is obvious that the surface N content of the mesoporous TiO_2 was considerably higher than that of the commercial Degussa P-25 TiO_2 at all preparation conditions, because of higher surface area of the mesoporous TiO_2, as well as other physical surface properties originating from specific preparation technique.

4.3 Photocatalytic H_2 Evolution Activity of N-doped TiO_2 Photocatalyst

The results of photocatalytic H_2 evolution over the photocatalysts are shown in Table 4.4 and Figures 4.12 and 4.13. The photocatalytic activity in the absence of either light irradiation, photocatalyst, or methanol was also comparatively studied. It was found that there was no detectable H_2 evolution in the absence of them, indicating that all of them are necessarily important for the photocatalytic H_2 evolution. It can be seen from Table 4.4 and Figure 4.12 that the N-doped mesoporous TiO_2 with the urea:TiO_2 molar ratio of 1:1 prepared at calcination temperature of 250°C exhibited the highest H_2 evolution activity. For the series of widely known high photocatalytic activity commercial Degussa P-25, the best N-doping conditions were the urea:TiO_2 molar ratio of 0.5:1 and the calcination temperature of 250°C, as shown in Table 4.4 and Figure 4.13.

At 200 and 250°C, the photocatalytic H_2 evolution activity of N-doped mesoporous TiO_2 tended to increase with increasing the urea:TiO_2 molar ratio to from 0.5:1 to 1:1 and then decrease with further increasing the molar ratio. It seems that for the N-doped mesoporous TiO_2 with the urea:TiO_2 molar ratio of 3:1, a huge amount of urea was decomposed to biuret (at 200 and 250°C) and further to cyanuric acid (250°C), and they could not be completely removed and were consequently left inside the mesoporous structure, as shown in XRD patterns (Figure 4.9(d), (g), and (j)). The biuret and cyanuric acid are comparatively large molecule, so the pore of mesoporous TiO_2 could be easily blocked, resulting in the decreased H_2 evolution activity due to the less accessability of the reactants to the photocatalyst surface (Table 4.2 and 4.4) despite higher surface N content (Table 4.3). At 300°C, the photocatalytic activity tendency of N-doped mesoporous TiO_2 was different from the other two calcination temperatures. The H_2 evolution gradually decreased as the molar ratio further increased. A possible explanation might be that at this temperature, higher amount of biuret formed can be more easily decomposed to gas phase, as well as be transformed to cyanuric acid. The surface nitrogen may then also be more released, resulting in less N content and subsequent lower photocatalytic activity observed, as shown in Table 4.3. In addition, although the cyanuric acid formation at the molar ratio of 1:1 was not observed from XRD results, but the results of decreased pore volume and increased amount of N content can be confirmed, as shown in Table 4.2 and 4.3.

Table 4.4 Photocatalytic H_2 evolution results over the photocatalysts (Reaction conditions: photocatalyst, 0.2 g; distilled water, 150 ml; methanol, 50 ml; and irradiation time, 5 h)

Photocatalyst	Calcination temperature /°C	Urea:TiO_2 molar ratio	H_2 evolution /$\mu l h^{-1}$
Synthesized mesoporous TiO_2	200	0.5:1	1.33
		1:1	1.74
		3:1	0.17
	250	0.5:1	3.91
		1:1	6.23
		3:1	0.42
	300	0.5:1	5.10
		1:1	1.72
		3:1	0.61
Degussa P-25 TiO_2	200	0.5:1	3.59
		1:1	4.10
		3:1	0.27
	250	0.5:1	4.37
		1:1	2.07
		3:1	0.65
	300	0.5:1	0.68
		1:1	0.56
		3:1	0.56
No light irradiation			-
No photocatalyst			-
No methanol			-

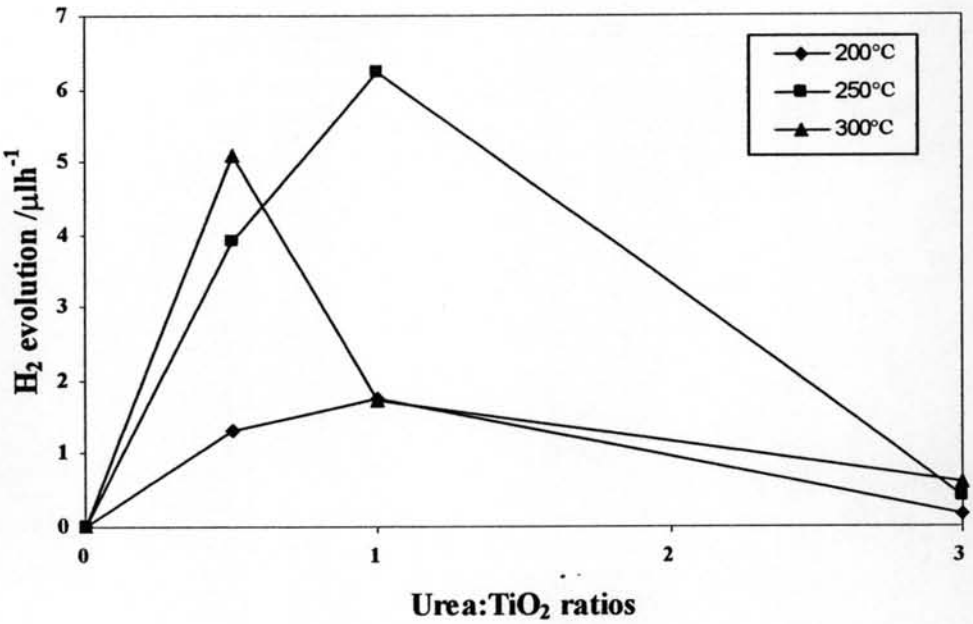

Figure 4.12 The H_2 evolution of N-doped mesoporous TiO_2 with different urea:TiO_2 molar ratios of 0.5:1, 1:1, and 3:1 prepared at different calcination temperatures of 200, 250, and 300°C.

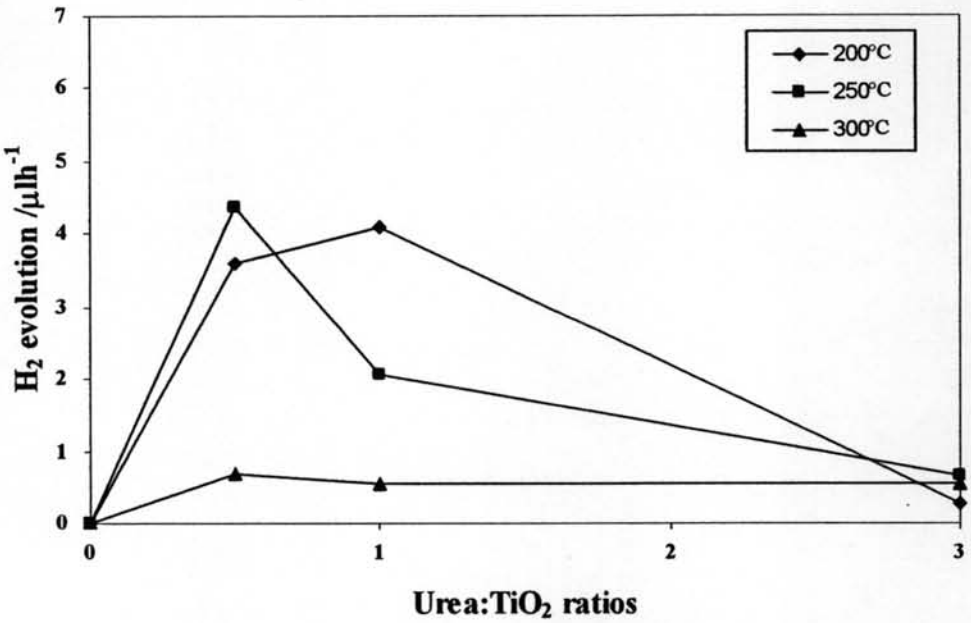

Figure 4.13 The H_2 evolution of N-doped commercial Degussa P-25 TiO_2 with different urea:TiO_2 molar ratios of 0.5:1, 1:1, and 3:1 prepared at different calcination temperatures of 200, 250, and 300°C.

For the H_2 evolution of N-doped commercial Degussa P-25 photocatalysts, at 200°C, the photocatalytic H_2 evolution activity tended to increase with increasing the urea:TiO_2 molar ratio from 0.5:1 to 1:1 and then decrease with further increasing the molar ratio. At 250°C, the H_2 evolution gradually decreased as the molar ratio further increased. At 300°C, the H_2 evolution remained almost unchanged, even though the molar ratio increased. Their activity is quite different from the N-doped mesoporous TiO_2 ones. It seems to be that the pore size is considerably important, affecting to H_2 evolution activity. As previously mentioned, the pore size of commercial Degussa P-25 TiO_2 is mostly in the range of macropore region, of which pore size is greater than 50 nm in diameter. According to the extremely large pore size of the commercial Degussa P-25 TiO_2, this means that it possessed much more empty space in the pore structure than the mesoporous TiO_2. This might lead to much easier conversion of biuret (straight chain compound) to cyanuric acid (cyclic compound) according to Eq. 17. This effect is relatively dominant at high temperatures (250 and 300°C) because the biuret can be comfortably transformed to cyanuric acid or even released into gas phase, resulting in the less H_2 evolution activity. At the calcination temperature of 300°C, in addition to the previous reason, the surface N content is another important parameter, which could be related to the constant H_2 evolution activity. From the results of surface N content (Table 4.3), the surface N content at 300°C was less than that at the other calcination temperatures and not quite different between the urea:TiO_2 molar ratios of 0.5:1 and 1:1, resulting in the almost unchanged H_2 evolution activity. Moreover, even though the surface N content of the photocatalyst with urea:TiO_2 molar ratio of 3:1 increased, the photocatalytic H_2 evolution activity was negatively affected by its relatively low surface area.

4.4 Pt-Loaded N-Doped Mesoporous TiO_2 Characterizations and Photocatalytic Activity

In order to understand the role of Pt, the brief mechanism of photocatalytic H_2 evolution over Pt/TiO_2 is first explained. The reaction is initiated by the photoexcitation of TiO_2 particles, which leads to the formation of electron hole pairs. Photogenerated conduction band electrons can be transferred to electron acceptor, H^+. With Pt on TiO_2 photocatalyst, Pt can rapidly trap electrons, and hydrogen can be produced on Pt by reduction reaction. Likewise, valence band holes can be filled by the electron donor, CH_3OH, resulting in the great prevention of photoinduced charge recombination (Kawai *et al.*, 1980 and Bamwenda *et al.*, 1995).

Since, among all the investigated photocatalysts, the N-doped mesoporous TiO_2 with the urea:TiO_2 molar ratio of 1:1 prepared at calcination temperature of 250°C showed the highest photocatalytic activity, it was taken to study the effects of Pt cocatalyst loading in order to improve the H_2 evolution activity of the system. The Pt was loaded onto the TiO_2 photocatalyst by using incipient wetness impregnation method. The XRD results of the N-doped mesoporous TiO_2 with various Pt loading content are shown in Figure 4.14.

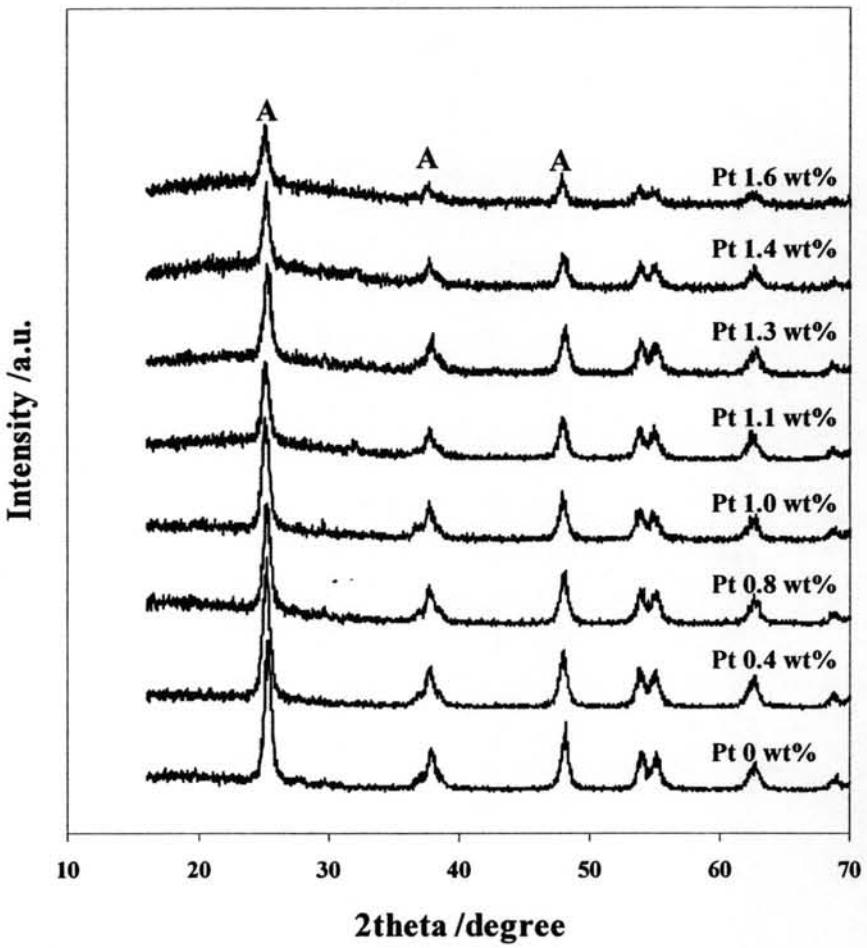

Figure 4.14 XRD patterns of Pt-loaded N-doped mesoporous TiO_2 with molar ratios of urea:mesoporous TiO_2 of 1:1 at calcination temperature of 250°C (A: Anatase TiO_2).

The XRD diffactograms of Pt-loaded samples are not quite different form pure mesoporous TiO_2. From the XRD result, the indistinguishable presence of the diffraction peaks of Pt at 39.8° indexed to (1 1 1) plane indicates that the Pt particles were in a very high dispersion degree. As the minimum detection limit of the XRD technique is around 5 nm, it is inferred that the crystallite size of the Pt particles was below that value. From TEM image of 1.3 wt% Pt-loaded N-doped mesoporous TiO_2 as shown in Figure 4.15, it is evident that the nanocrystalline TiO_2 aggregates was formed with three dimensional disordered primary particles. The observed TiO_2 particle size of 10–15 nm is in good accordance with the crystallite size of 13.6 nm

estimated from XRD line broadening, elucidating that each grain can be reliably considered in average as a single crystal. From visualization of the image, dark patch indicates high electron density, and it corresponds to the deposition of Pt nanoparticle with different crystallographic lattice fringes and their orientations from that of TiO_2 nanoparticle. The particle size of Pt was observed to be approximately 5 nm, which certainly corresponds to the result of XRD diffractogram.

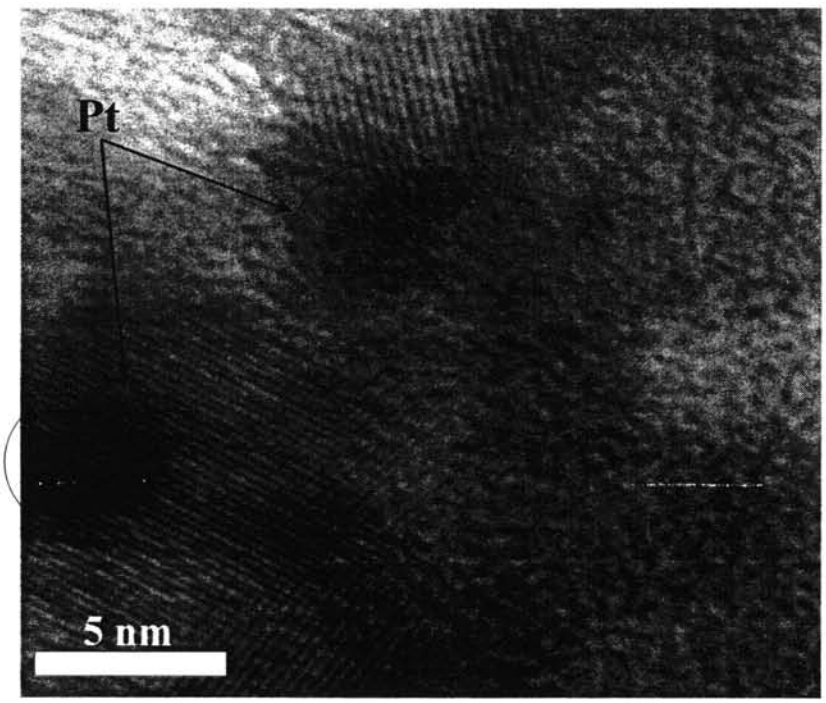

Figure 4.15 TEM image of 1.3 wt% Pt-loaded N-doped mesoporous TiO_2 prepared by incipient wetness impregnation method at calcination temperature of 200°C for 6 h.

To explore the Pt content on the photocatalyst surface, XPS analysis was also performed, as exemplified in Figure 4.16.

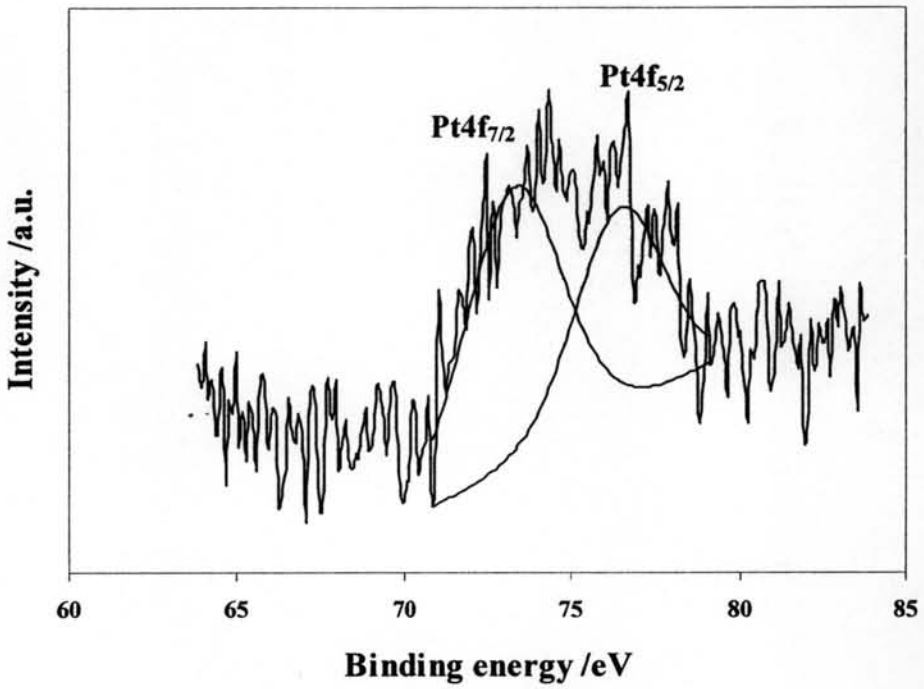

Figure 4.16 XPS spectrum of Pt4f for 1.3 wt% Pt-loaded N-doped mesoporous TiO_2.

The Pt4f spectrum appeared at 73.3 and 76.4 eV for $Pt4f_{7/2}$ and $Pt4f_{5/2}$, respectively, which can be denoted to Pt oxides at high oxidation state (Zhang *et al*, 2006). The peak intensity is considerably low and very difficult to be visible observed due to low nominal Pt loading. The surface content and corresponding H_2 evolution activity at various nominal Pt loading content are shown in Table 4.5.

Table 4.5 Summary of the effect of Pt loading onto N-doped mesoporous TiO_2 on surface Pt content and photocatalytic H_2 evolution (Reaction conditions: photocatalyst, 0.2 g; distilled water, 150 ml; methanol, 50 ml; and irradiation time, 5 h)

Nominal Pt loading /wt%	Surface Pt content /wt%	H_2 evolution /μlh^{-1}
0	0	6.23
0.4	0.80	8.05
0.8	3.69	15.19
1.0	3.23	17.89
1.1	3.30	17.95
1.3	4.73	26.40
1.4	3.25	11.75
1.6	3.71	8.04

It can be seen that the surface Pt content increased with increasing the nominal Pt loading content up to 1.3 wt%, and then beyond this loading content, the suitably surface Pt content decreased probably due to the agglomeration of some Pt nanoparticles. This result could be suitably related to the H_2 evolution activity. The results clearly reveal that the H_2 evolution activity also reached a maximum at the nominal Pt loading content of 1.3 wt%. This can be explained in that with the initial increase in the Pt loading content, TiO_2 particles may carry more Pt nanoclusters, which are indispensable for the removal of photogenerated electrons from TiO_2 for the reduction reaction, leading to an increase of the photocatalytic activity. After reaching a maximum, the decrease in the activity with further increase in the Pt content beyond a certain optimum value may be, at least partly, due to too much Pt nanoclusters on TiO_2. These clusters would shield the photosensitive TiO_2 surface, scatter the visible light to decrease the absorption by TiO_2, and subsequently diminish the surface concentration of the electrons and holes available for the reactions. Another explanation is that at high metal loadings, the deposited metal

particles may act as the recombination centers for the photoinduced species (Courbon *et al.*, 1984).